

Single-shot initialization of electron spin in a quantum dot using a short optical pulse

Vivien Loo,¹ Loïc Lanco,^{1,2,*} Olivier Krebs,¹ Pascale Senellart,¹ and Paul Voisin¹

¹Laboratoire de Photonique et Nanostructures, LPN/CNRS, Route de Nozay, F-91460 Marcoussis, France

²Université Paris Diderot–Paris 7, UFR de Physique, 4 rue Elsa Morante, F-75205 Paris CEDEX 13, France

(Received 2 December 2010; published 10 January 2011)

We propose a technique to initialize an electron spin in a semiconductor quantum dot with a single short optical pulse. It relies on the fast depletion of the initial spin state followed by a preferential, Purcell-accelerated deexcitation toward the desired state thanks to a micropillar cavity. We theoretically discuss the limits on initialization rate and fidelity and derive the pulse area for optimal initialization. We show that spin initialization is possible using a single optical pulse down to a few tens of picoseconds wide.

DOI: [10.1103/PhysRevB.83.033301](https://doi.org/10.1103/PhysRevB.83.033301)

PACS number(s): 78.67.Hc, 03.67.Lx, 42.50.Pq, 78.47.—p

Semiconductor quantum dots (QDs) constitute good candidates for the implementation of quantum information processing in the solid state. In the last ten years, the coupling of a single QD transition to an optical cavity mode has allowed numerous cavity quantum electrodynamics realizations, in both the weak and strong coupling regimes.^{1–5} To benefit from the microsecond spin coherence time,⁶ for an electron trapped in a quantum dot, spin qubit initialization,^{7–9} manipulation,^{10,11} and readout^{12,13} are also being widely explored. At the interface, several proposals have focused on the use of light-matter coupling to achieve remote qubit entanglement.^{14,15} Here the potential of cavity-QD systems for short-pulse spin initialization is explored.

High-fidelity electron spin state preparation has been obtained by several groups worldwide, using different configurations: magnetic field oriented parallel⁷ or perpendicular^{8,9} to the optical beam for electron spin initialization. Only the perpendicular (Voigt) geometry allows initialization times shorter than the typical spin coherence time: as shown by Emary *et al.*,⁸ an initialization fidelity of 99% can be reached in approximately 5 ns in such a configuration. In this Brief Report we show that spin initialization can be performed with a single optical pulse down to a few tens of picoseconds wide, using a QD coupled to a high-quality-factor (Q) optical cavity mode, such as the QD-micropillar system sketched in Fig. 1(a).

The corresponding four-level system, in Voigt geometry, is shown in Fig. 1(b): the low-energy levels are the Zeeman-split electron states with spins along the x axis, that is, $|e^\pm\rangle = (|\uparrow\rangle \pm |\downarrow\rangle)/\sqrt{2}$, where $|\uparrow\rangle$ and $|\downarrow\rangle$ denote the electron spin states quantized along the z axis. The high-energy levels are the Zeeman-split trion states $|t^\pm\rangle = (|\uparrow\rangle|\downarrow\rangle - |\downarrow\rangle|\uparrow\rangle) / \sqrt{2}$, where $|\uparrow\rangle$ and $|\downarrow\rangle$ denote the heavy-hole spin states in the z direction. In the case of pure heavy-hole states, the $|t^+\rangle \rightarrow |e^+\rangle$ and $|t^-\rangle \rightarrow |e^-\rangle$ transitions are X polarized (linearly polarized parallel to the magnetic field), while the $|t^+\rangle \rightarrow |e^-\rangle$ and $|t^-\rangle \rightarrow |e^+\rangle$ transitions are Y polarized (perpendicular to the magnetic field).⁸ We consider a cavity mode in resonance with the $|t^+\rangle \rightarrow |e^-\rangle$ transition, accelerating emission in the mode by a Purcell factor F_p .

The initialization process described in Ref. 8 relies on the resonant excitation of the $|t^+\rangle \rightarrow |e^+\rangle$ transition by an X -polarized laser: the system can then either relax into the desired state $|e^-\rangle$ or return to $|e^+\rangle$, where it can be excited once again. The population remaining in $|e^+\rangle$ thus decreases

exponentially with a characteristic time τ , given in this case by $\frac{2}{\Gamma}$ where Γ is the spontaneous emission rate of the electron-trion transitions. Near-unity fidelity initialization can thus be obtained using optical pulses of durations Δt such that $\Delta t \gg \tau$.

Here we show that the selective Purcell acceleration of the $|t^+\rangle \rightarrow |e^-\rangle$ transition not only decreases the value of this characteristic time down to $\tau = \frac{2}{(F_p+1)\Gamma}$, but also allows initialization with optical pulses of durations Δt shorter than τ . In this regime the initialization process can be schematically viewed as a two-step procedure: complete depletion of $|e^+\rangle$ toward $|t^+\rangle$ using a pulse of carefully controlled area, followed by a preferential, Purcell-accelerated relaxation toward $|e^-\rangle$. In the following we analyze the initialization rate and fidelity, and derive the pulse area required for optimal spin initialization. We finally show that micropillar-QD systems with the required properties can be realized using state-of-the-art fabrication techniques.

We consider an X -polarized laser field applied in resonance with $|e^+\rangle \rightarrow |t^+\rangle$; the second X -polarized transition is detuned by an amount Σ_B from the laser field frequency. The laser being nonresonant with the optical mode, the coupling with these transitions occurs mainly through the pillar leaky modes, so that we can assume an equal pumping rate Ω for both of them. We thus use the Hamiltonian given by Emary *et al.*,⁸ except that we define Ω as the Rabi frequency of the resonantly driven transition, which is twice higher than their definition.

We determine the properties of our system by solving the master equation for the density matrix ρ in the Linblad form ($\hbar = 1$ units).⁸ We assume for simplicity that the Purcell effect only alters the spectrally matched $|t^+\rangle \rightarrow |e^-\rangle$ transition whose total spontaneous emission rate becomes $(F_p + 1)\Gamma$ (that is, $F_p\Gamma$ in the cavity mode, and Γ in the micropillar leaky modes), the other decay rates remaining equal to Γ . We thus use the Lindblad operators of Ref. 8, with the same value $\Gamma = 1.2 \mu\text{eV}$ ($\Gamma^{-1} = 0.55$ ns), except for a term $(F_p + 1)\Gamma$ instead of Γ for the accelerated transition.

We first consider a continuous-wave (cw) pumping rate Ω instantaneously switched on at time $t = 0$. In the high- Σ_B limit, the varying terms in the Hamiltonian oscillate so rapidly that their contribution is averaged to zero, and the density matrix elements $\rho_{ij}(t)$ tend toward constant values $\rho_{ij}^{(0)}$ which are all equal to zero except for $\rho_{e^+e^+}^{(0)} = 1$. In the long-time limit, the differences $\rho_{ij}(t) - \rho_{ij}^{(0)}$ decrease proportionally to e^{-t/τ_0} ,

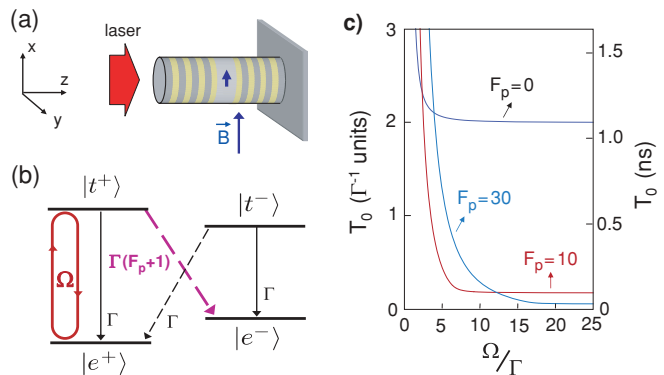


FIG. 1. (Color online) (a) QD-micropillar device in Voigt geometry. (b) Four-level system and corresponding optical transitions (solid line, X polarized; dashed line, Y polarized), with Ω and Γ the pumping and relaxation rates, respectively. (c) Initialization time T_0 for $F_p = 0, 10$, and 30 as a function of Ω/Γ .

where the initialization time T_0 can be determined analytically. Adapting the calculation of Emary *et al.*⁸ to take into account the Purcell acceleration, we find a more general form for T_0 as a function of the ratio $r = \frac{\Omega}{\Gamma}$: $T_0 = \Gamma^{-1}[\alpha - \mu^{1/3} - \beta\mu^{-1/3}]^{-1}$, using $\alpha = 1 + \frac{F_p}{2}$, $\beta = \frac{\alpha^2 - r^2}{3}$ and $\mu = (\frac{r}{2})^2 + \sqrt{(\frac{r}{2})^4 - \beta^3}$.

The evolution of T_0 is shown in Fig. 1(c): as expected, the initialization time is greatly shortened by the Purcell acceleration of the $|t^+ \rangle \rightarrow |e^- \rangle$ transition. For high enough values of Ω ($r \gg F_p + 1$), an asymptotic regime is reached where T_0 tends toward the characteristic time $\tau = \frac{2}{(F_p+1)\Gamma}$; in this regime the initialization speed is not limited by the pumping rate but solely by the deexcitation rate of $|t^+ \rangle$ toward $|e^- \rangle$. The time required to obtain 99% initialization fidelity is approximately $5T_0$, which is at best $10\Gamma^{-1}$ in the case $F_p = 0$ (no cavity), but decreases to $0.25\Gamma^{-1}$ when $F_p = 40$.

If we now reckon with the complete time-dependent Hamiltonian (finite Σ_B), we find that an undesired population will always remain in the state $|e^+ \rangle$. This arises from the residual Rabi oscillation in the nonresonantly driven, X-polarized transition from $|e^- \rangle$ to $|t^- \rangle$. This oscillation, with a generalized Rabi frequency $\sqrt{\Omega^2 + \Sigma_B^2}$ and an amplitude proportional to $\frac{\Omega}{\sqrt{\Omega^2 + \Sigma_B^2}}$, allows a relaxation from $|t^- \rangle$ to $|e^+ \rangle$. To determine the corresponding populations, we remark that in the long-time limit the density matrix elements $\rho_{ij}(t)$ still tend toward constants $\rho_{ij}^{(0)}$, except for $\rho_{e^-t^-}$ which tends toward $q e^{-i\Sigma_B t}$, with q a complex number. Injection of these matrix elements into the master equation leads to the determination of the asymptotic values for the populations $\rho_{ii}^{(0)}$:

$$\rho_{e^+e^+}^{(0)} = [(F_p + 2)^2\Gamma^2 + \Omega^2]/D, \quad (1)$$

$$\rho_{e^-e^-}^{(0)} = 1 - [(F_p + 2)^2\Gamma^2 + (F_p + 3)\Omega^2]/D, \quad (2)$$

$$\rho_{t^+t^+}^{(0)} = \Omega^2/D, \quad (3)$$

$$\rho_{t^-t^-}^{(0)} = (F_p + 1)\Omega^2/D, \quad (4)$$

with the denominator D given by

$$D = (8 + 8F_p + F_p^2)\Gamma^2 + 4(F_p + 1)\Sigma_B^2 + 2(F_p + 2)\Omega^2. \quad (5)$$

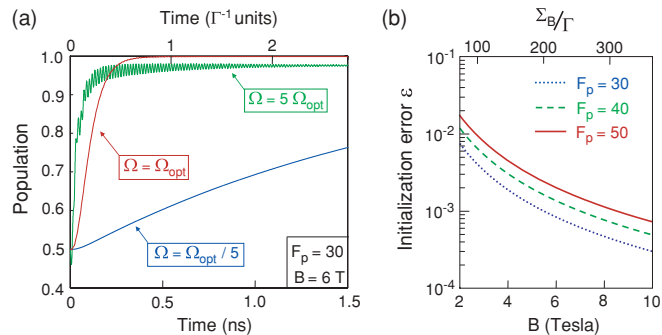


FIG. 2. (Color online) (a) Population of $|e^- \rangle$ as a function of time, numerically integrated for $F_p = 30$ and $B = 6 T$, using different pumping rates around the optimal value $\Omega_{\text{opt}} = (F_p + 1)\Gamma/2$. (b) Final initialization error as a function of the magnetic field, for $F_p = 30, 40$, and 50 , for the optimal pumping rate.

The residual population in $|e^+ \rangle$ is an increasing function of the pumping rate Ω ; thus, once the latter is set to an appropriate value for fast spin initialization, raising it becomes counterproductive. We find that choosing $\Omega_{\text{opt}} = \frac{1}{\tau} = \frac{(F_p+1)\Gamma}{2}$ as the optimal pumping rate provides a good compromise between initialization speed and fidelity. Figure 2(a) shows the evolution of $\rho_{e^-e^-}(t)$ for various pumping rates, with $F_p = 30$ and $B = 6 T$ magnetic field, with Σ_B determined using the electron and hole transverse g factors $g_{\perp}^e = -0.46$ and $g_{\perp}^h = -0.29$.⁸ A pumping rate significantly lower than Ω_{opt} slows the initialization rate; a higher pumping rate enhances the residual Rabi oscillations in the $|e^- \rangle \rightarrow |t^- \rangle$ transition.

We now calculate the corresponding initialization error, assuming the cw laser field is turned off at time $t = \Delta t$ with $\Delta t \gg \tau$, so that at the end of the pulse the populations have already converged toward their asymptotic values $\rho_{ii}^{(0)}$. At the end of the optical pulse, the population remaining in the state $|t^+ \rangle$ relaxes toward $|e^+ \rangle$ with probability $\frac{1}{F_p+2}$ and toward the desired state $|e^- \rangle$ with probability $\frac{F_p+1}{F_p+2}$. Similarly, the population in the trion state $|t^- \rangle$ relaxes toward $|e^+ \rangle$ and $|e^- \rangle$ with probabilities $\frac{1}{2}$. Thus the initialization error we consider is the residual population in $|e^+ \rangle$ after the pulse, given by $\rho_{e^+e^+}^{(\infty)} = \rho_{e^+e^+}^{(0)} + \frac{1}{F_p+2}\rho_{t^+t^+}^{(0)} + \frac{1}{2}\rho_{t^-t^-}^{(0)}$. We denote by ϵ this final initialization error, which is found to be

$$\epsilon = \frac{2(F_p + 2)^2\Gamma^2 + \frac{8+5F_p+F_p^2}{F_p+2}\Omega^2}{D}. \quad (6)$$

In Fig. 2(b), ϵ is plotted as a function of the magnetic field for various Purcell factors, using the optimal pumping rate Ω_{opt} . The error increases when F_p increases, due to the higher value of Ω_{opt} . As expected, the obvious way to limit the initialization error is to increase Σ_B in the denominator D , and thus the magnetic field.

A major feature of the present initialization procedure, however, is that the practical implementation of spin initialization does not require a pulse duration Δt higher than τ . A short optical pulse of carefully controlled area can indeed transfer the population from the $|e^+ \rangle$ state to the $|t^+ \rangle$ state; in a second step, the preferential, Purcell-accelerated relaxation of $|t^+ \rangle$ leads to a nearly complete initialization in $|e^- \rangle$. For this method

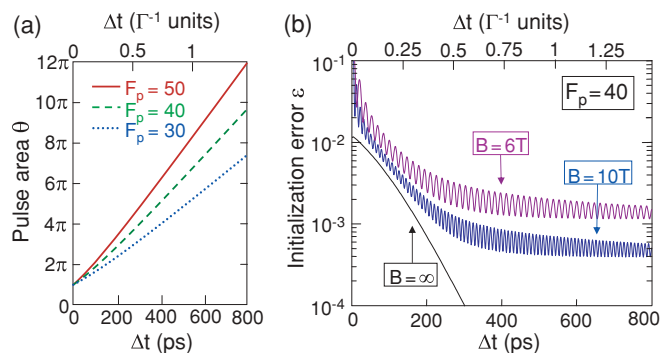


FIG. 3. (Color online) (a) Pulse area for optimal initialization for $F_p = 30, 40$, and 50 , as a function of the square pulse duration, as deduced from Eq. (8). (b) Initialization error corresponding to this pulse area, for $B = 6$ and 10 T, and in the limit of infinite magnetic field, with a Purcell factor $F_p = 40$.

to work, a strong Purcell factor is needed, so that the transition back to $|e^+\rangle$ is quenched as much as possible. The second issue is that, for the unintended $|e^-\rangle \rightarrow |t^-\rangle$ transition to remain unaffected by the laser pulse, Σ_B must be much higher than the laser spectral width.

To calculate the required pulse area for optimal initialization, we consider the case of a square optical pulse with a constant pumping rate Ω , in the limit $F_p \gg 1$ and Σ_B much greater than both $\frac{1}{\Delta t}$ and $\frac{1}{\tau}$. In such a case, with the laser field switched on at $t = 0$, the population of the $|e^+\rangle$ state simply evolves as

$$\frac{\rho_{e^+e^+}(t)}{\rho_{e^+e^+}(0)} = \left[\frac{\Omega^2}{2\lambda^2} + \left(1 - \frac{\Omega^2}{2\lambda^2}\right) \cos \lambda t + \frac{\sin \lambda t}{\lambda \tau} \right] e^{-\frac{t}{\tau}} \quad (7)$$

with $\lambda = \sqrt{\Omega^2 - (\frac{1}{\tau})^2}$. We remark that $\rho_{e^+e^+}$ reaches zero at the end of the optical pulse if the latter's duration and pumping rate are related by

$$\arctan \lambda \tau + \frac{\lambda \Delta t}{2} = \pi. \quad (8)$$

The corresponding pulse area, $\theta = \Omega \Delta t$, can be deduced by numerical solving of Eq. (8).

Figure 3(a) shows this pulse area for various Purcell factors, as a function of the pulse duration. The limit $\Delta t \ll \tau$ leads to a pulse area $\theta = \pi$ for complete depletion: this is a well-known property of two-level systems, valid as long as the pulse duration is negligible with respect to the relaxation times. For longer pulses, however, the required area increases with Δt . When $\Delta t \gg \tau$ an asymptotic behavior is obtained where $\theta \approx \frac{\Delta t}{\tau}$. This corresponds to $\Omega \approx \frac{1}{\tau}$, which is the above-mentioned optimal pumping rate $\Omega_{\text{opt}} = \frac{(F_p+1)\Gamma}{2}$.

If this optimal pulse area is used, the limit $F_p \gg 1$ ensures that the population excited in $|t^+\rangle$ relaxes toward $|e^+\rangle$ only, leading to a perfect spin initialization. In practice, however, the finite values of the Purcell factor and magnetic field lead to a nonzero initialization error, which we investigate numerically. Figure 3(b) plots the initialization error as a function of pulse duration, for 6 T, 10 T, and infinite magnetic fields, using $F_p = 40$. As expected, for pulse durations $\Delta t \gg \tau$ the errors converge toward the values described in Fig. 2(b), as given by Eq. (6) for $\Omega = \frac{1}{\tau} = \frac{(F_p+1)\Gamma}{2}$. The oscillatory behavior

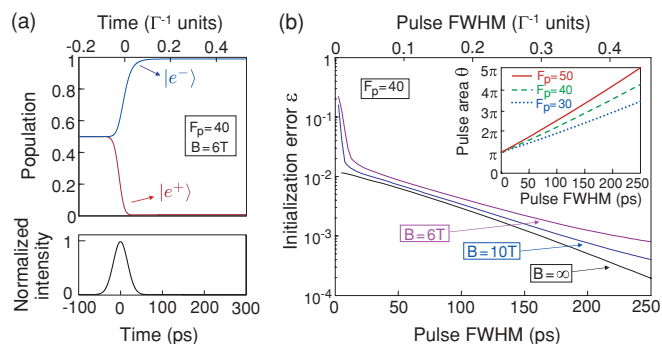


FIG. 4. (Color online) (a) Optical-pulse normalized intensity and corresponding populations of $|e^+\rangle$ and $|e^-\rangle$ states, as a function of time (40 ps FWHM Gaussian pulse, with $F_p = 40$ and $B = 6$ T). (b) Initialization error as a function of the Gaussian pulse width for 6 T, 10 T, and infinite magnetic fields, with $F_p = 40$. Inset: Required pulse area for optimal initialization using a Gaussian pulse, for $F_p = 30, 40$, and 50 .

arises from the nonadiabatic switching of the laser field at $t = 0$ and $t = \Delta t$: as shown in Fig. 2(a), this leads to residual Rabi oscillations in the $|e^-\rangle \rightarrow |t^-\rangle$ transition. In the limit of a very short pulse and for an infinite magnetic field, the initialization error tends toward

$$\epsilon_{\Delta t \rightarrow 0, B \rightarrow \infty} = \rho_{e^+e^+}(0) \frac{1}{F_p + 2}, \quad (9)$$

which is the population transferred from $|e^+\rangle$ to $|t^+\rangle$ multiplied by the probability of the unwanted relaxation from $|t^+\rangle$ back to $|e^+\rangle$. However, in this regime, and for realistic magnetic fields, the condition $\Sigma_B \Delta t \gg 1$ is no longer satisfied: the high spectral width of the pumping laser precludes any efficient initialization, as the $|e^-\rangle \rightarrow |t^-\rangle$ transition is strongly excited.

For these short optical pulses, the approximation of a square pulse is often inappropriate; yet the validity of the method does not depend on the pulse shape as long as the pulse area $\theta = \int \Omega(t) dt$ is carefully controlled. Figure 4(a) shows the numerical calculation of the $|e^+\rangle$ and $|e^-\rangle$ populations for a 6 T magnetic field and an $F_p = 40$ Purcell factor, using a Gaussian pulse with a 40 ps ($0.07\Gamma^{-1}$) full width at half maximum (FWHM). In such a case the magnetic field is high enough to ensure that the unintended $|e^-\rangle \rightarrow |t^-\rangle$ transition is nonresonant with the laser pulse, which results in the absence of depletion of the $|e^-\rangle$ state during the pulse. The preferential relaxation toward $|e^-\rangle$ leads to a final initialization fidelity around 99%, measured at time $t = 140$ ps ($0.25\Gamma^{-1}$); the initialization process is thus approximately 40 times faster than without a cavity. To achieve such a fidelity with a 20 ps FWHM pulse, a Purcell factor $F_p = 50$, and a magnetic field $B = 10$ T are required.

Figure 4(b) shows the expected initialization error for 6 T, 10 T, and infinite magnetic fields, using $F_p = 40$. As expected, the initialization error in the limit of infinite magnetic field and very short pulse duration remains given by Eq. (9). The main difference from Fig. 3(b) is that the smooth evolution of $\Omega(t)$ allows a monotonic decrease of the initialization error when the pulse width increases. As long as the pulse FWHM is larger than a few tens of picoseconds, thanks to the limited spectral

width of the Gaussian pulse, the finite value of the magnetic field does not significantly alter the initialization efficiency.

The inset of Fig. 4(b) summarizes the required pulse area, as a function of the pulse FWHM, displaying the same behavior as in Fig. 3(a) for square pulses: the pulse area for optimal initialization grows above π when the pulse width increases. We note that the pulse area shows no significant dependence on the magnetic field in the 6–10 T range, and that no fine-tuning is required for practical implementation: for example, a 2% shift of the pulse area will result in an increase of the initialization error of the order of a few 10^{-3} .

We now show that this spin initialization procedure can be implemented in realistic QD-cavity systems. The current state of the art of nanofabrication techniques allows the realization, in a way both deterministic and scalable, of QD-micropillar systems whose cavity mode is spatially and spectrally matched with a selected QD transition.¹⁶ Micrometer-sized pillars can be realized with quality factors up to 10^5 .¹⁷ For example, a 3- μm -diameter AlAs/GaAs micropillar (effective mode volume $V \approx 1 \mu\text{m}^3$ and effective index $n \approx 3.4$) with a quality factor $Q = 2.5 \times 10^4$, embedding a single InAs/GaAs QD with $f = 10$ oscillator strength (transition wavelength $\lambda = 0.94 \mu\text{m}$) will present a Purcell factor $F_p \approx 40$ while staying in the weak-coupling regime.³

A key condition for the validity of this initialization procedure is that the undesired relaxation from $|t^+\rangle$ back to $|e^+\rangle$ does not experience any significant Purcell acceleration. Using the transverse g factors of Ref. 8, we find that a 6 T magnetic field

corresponds to a 160 μeV detuning between the $|t^+\rangle \rightarrow |e^+\rangle$ transition and the cavity mode, whereas the mode resonance half-width is 25 μeV for $Q = 2.5 \times 10^4$: this corresponds to a Purcell factor $F'_p \approx 1$ ($F'_p \approx 0.3$ for $B = 10$ T). The small Purcell effect experienced by the Y -polarized $|t^-\rangle \rightarrow |e^+\rangle$ transition (the Zeeman splitting between the Y -polarized transitions is only 60 μeV for $B = 6$ T) does not alter the validity of the method.

We also point out that the presence of heavy-hole–light-hole mixing in the QD can affect the trion states, resulting in a rotation of the polarization axis in the x - y plane;⁹ furthermore, a small alteration of the beam polarization may also occur in the Bragg mirrors, due to the residual ellipticity of the micropillar (ellipticities of the order of 5×10^{-4} are the current state of the art¹⁷). For simplicity the orthogonal polarization states of the optical transitions have been called X and Y , whether or not they correspond to linear polarizations along the x and y axes of Fig. 1(a). For efficient spin initialization the laser polarization has to be adjusted to ensure negligible excitation of the Y -polarized transitions.

Having derived the optical pulse area required for optimal initialization, as well as the corresponding fidelity and experimental conditions, we conclude that spin initialization can be implemented using short optical pulses down to a few tens of picoseconds wide.

This work is partially supported by ANR Project No. ANR-JCJC-09-0136.

*loic.lanco@lpm.cnrs.fr

¹C. Santori, D. Fattal, J. Vučković, G. S. Solomon, and Y. Yamamoto, *Nature (London)* **419**, 594 (2002).

²A. Dousse, J. Suffczyński, A. Beveratos, O. Krebs, A. Lemaître, I. Sagnes, J. Bloch, P. Voisin, and P. Senellart, *Nature (London)* **466**, 217 (2010).

³J. P. Reithmaier, G. Şek, A. Löffler, C. Hofmann, S. Kuhn, S. Reitzenstein, L. V. Keldysh, V. D. Kulakovskii, T. L. Reinecke, and A. Forchel, *Nature (London)* **432**, 197 (2004).

⁴T. Yoshie, A. Scherer, J. Hendrickson, G. Khitrova, H. M. Gibbs, G. Rupper, C. Ell, O. B. Shchekin, and D. G. Deppe, *Nature (London)* **432**, 200 (2004).

⁵E. Peter, P. Senellart, D. Martrou, A. Lemaître, J. Hours, J. M. Gerard, and J. Bloch, *Phys. Rev. Lett.* **95**, 067401 (2005).

⁶A. Greilich, D. R. Yakovlev, A. Shabaev, A. L. Efros, I. A. Yugova, R. Oulton, V. Stavarache, D. Reuter, A. Wieck, and M. Bayer, *Science* **313**, 341 (2006).

⁷M. Atatüre, J. Dreiser, A. Badolato, A. Högele, K. Karrai, and A. Imamoglu, *Science* **312**, 551 (2006).

⁸C. Emary, X. Xu, D. G. Steel, S. Saikin, and L. J. Sham, *Phys. Rev. Lett.* **98**, 047401 (2007).

⁹X. Xu, Y. Wu, B. Sun, Q. Huang, J. Cheng, D. G. Steel, A. S. Bracker, D. Gammon, C. Emary, and L. J. Sham, *Phys. Rev. Lett.* **99**, 097401 (2007).

¹⁰E. D. Kim, K. Truex, X. Xu, B. Sun, D. G. Steel, A. S. Bracker, D. Gammon, and L. J. Sham, *Phys. Rev. Lett.* **104**, 167401 (2010).

¹¹D. Press, T. D. Ladd, B. Zhang, and Y. Yamamoto, *Nature (London)* **456**, 218 (2008).

¹²J. Berezovsky, M. H. Mikkelsen, O. Gywat, N. G. Stoltz, L. A. Coldren, and D. D. Awschalom, *Science* **314**, 1916 (2006).

¹³M. Atatüre, J. Dreiser, A. Badolato, and A. Imamoglu, *Nature Phys.* **3**, 101 (2007).

¹⁴F. Meier and D. D. Awschalom, *Phys. Rev. B* **70**, 205329 (2004).

¹⁵C. Y. Hu, W. J. Munro, J. L. O'Brien, and J. G. Rarity, *Phys. Rev. B* **80**, 205326 (2009).

¹⁶A. Dousse, L. Lanco, J. J. Suffczyński, E. Semenova, A. Miard, A. Lemaître, I. Sagnes, C. Roblin, J. Bloch, and P. Senellart, *Phys. Rev. Lett.* **101**, 267404 (2008).

¹⁷S. Reitzenstein, C. Hofmann, A. Gorbunov, M. Strauß, S. H. Kwon, C. Schneider, A. Löffler, S. Höfling, M. Kamp, and A. Forchel, *Appl. Phys. Lett.* **90**, 251109 (2007).